Article

Self-assembling particle-siloxane coatings for superhydrophobic concrete

Ismael Flores Vivian, Vahid Hejazi, Marina Kozhukhova, Michael Nosonovsky, and Konstantin Sobolev

ACS Appl. Mater. Interfaces, **Just Accepted Manuscript** • Publication Date (Web): 18 Nov 2013

Self-assembling particle-siloxane coatings for superhydrophobic concrete

*Ismael Flores-Vivian[1], Vahid Hejazi[2], Marina I. Kozhukhova[1], Michael Nosonovsky[*2] and Konstantin Sobolev[1]*

[1]Department of Civil Engineering and Mechanics
[2]Department of Mechanical Engineering
University of Wisconsin, Milwaukee, Wisconsin, 53201 USA
nosonovs@uwm.edu

Abstract

We report here, for the first time in the literature, a method to synthesize hydrophobic and superhydrophobic concrete. Concrete is normally a hydrophilic material, which significantly reduces the durability of concrete structures and pavements. To synthesize water-repellent concrete, hydrophobic emulsions were fabricated and applied on portland cement mortar tiles. The emulsion was enriched with the polymethyl-hydrogen siloxane oil hydrophobic agent as well as metakaolin (MK) or silica fume (SF) to induce the micro-roughness and polyvinyl alcohol (PVA) fibers to create a hierarchical surfaces. Various emulsion types were investigated by using different mixing procedures, and single- and double-layer hydrophobic coatings were applied. The emulsions and coatings were characterized with Optical Microscope and Scanning Electron Microscope (SEM), and their wetting properties, including the water contact angle (CA) and roll-off angle were measured. A theoretical model for coated and non-coated concrete, which can be generalized for other types of materials, was developed to predict the effect of surface roughness and composition on the CA. An optimized distance between the aggregates was found where the CA has the highest value. The maximal CA measured was 151° for the specimen with PVA fibers treated with SF based emulsion. Since water penetration is the main factor leading to concrete deterioration, hydrophobic water-repellent concretes have much longer durability then regular concretes and can have broad range of applications in civil and materials engineering.

KEYWORDS: contact angle, hydrophobic concrete, superhydrophobicity, hierarchical roughness

1. Introduction

Fabrication of hydrophobic concrete is a very important task for many applications. Concrete, a mixture of portland cement as binder, and water as well as aggregates as fillers, is a porous material with pores ranging in size from nanometers to millimeters. There are various pore types within the cement hydration products, including entrapped and entrained air voids up to a few millimeters in diameter, capillary pores in a range of a few micrometers in diameter and nanoscale gel pores. In most applications concrete surface is subjected to external erosion, abrasion and environmental exposure to aggressive liquids, such as water, mineral solutions, oil, solvents, etc. When dry concrete comes into contact with a liquid such as water, most of the water is absorbed by the pores due to the capillary forces. The capillary forces are dependent on the surface tension of the liquid (typically water), its contact angle (CA) with the pore walls, and the radius of the pores.[1] The durability (i.e. freeze-thaw and sulfate attack) of concrete depends on its overall absorption and permeability to aqueous solutions. For example, freeze-thaw damage occurs when water in saturated concrete freeze due to temperature fluctuations causing considerable stresses within the material. The cumulative effect of freeze-thaw cycles eventually cause expansion, cracking, scaling and crumbling of the concrete. It is therefore crucial to synthesize water-repellent concrete in order to increase its durability, and, in particular, to produce the ultra-durable concrete.[2]

The apparent CA is the principal parameter which characterizes the wetting properties of the surface.[3] When the CA is greater than 90^{o}, it indicates the hydrophobicity, while the CA less than 90° shows the hydrophilicity, which is the tendency of a surface to become wet or to absorb water, as shown in Figure 1. Common concrete is hydrophilic. The superhydrophobicity corresponds to apparent CA between 150° and 180°. Furthermore, not only high apparent CA but

low hysteresis of contact angle is necessary for true superhydrophobicity.[4-7] CA hysteresis is the difference between the advancing and receding CA and serves as a measure of adhesion between water and the solid substrate. Adhesion under various modes of loading can be also measured with the centrifugal adhesion balance.[8,9]

The surfaces that are not quite superhydrophobic, but exhibit high CA between 120° and 150°, which is above typical values for hydrophobic materials, are called sometimes "overhydrophobic." The water CA with a solid surface can be measured by goniometer or tensiometer. The CA of a water droplet on a smooth solid surface, θ_0, can be calculated by using the Young equation

$$\cos\theta_0 = \frac{\gamma_{SA}-\gamma_{SW}}{\gamma_{WA}} \quad (1)$$

where γ_{SW}, γ_{SA}, and γ_{WA} are the solid-water, solid-air, and water-air interfacial energies, respectively.

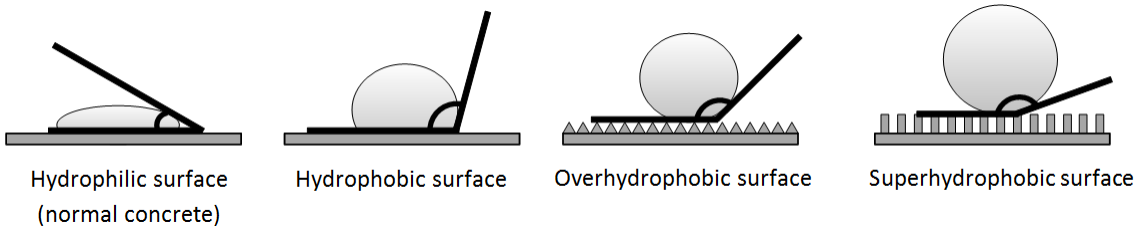

Figure 1. The hydrophilic ($0°\leq\theta\leq90°$), hydrophobic ($90°\leq\theta$), "over-hydrophobic" ($120°\leq\theta<150°$) and superhydrophobic ($150°\leq\theta\leq180°$) surfaces, where θ is the CA.

However, in practice, the surfaces are not quite smooth and usually possess micro- and nano-roughness. Two analytical models explaining the roughness effect on wetting properties of the surfaces were proposed by Wenzel[10] and Cassie-Baxter.[11] According to the Wenzel model,

wetting is homogeneous because water fills all pores and cavities at the surface (Fig. 2a). This model states that roughening a hydrophobic solid surface enhances its hydrophobicity by increasing the surface area:

$$\cos\theta = R_f \cos\theta_0 \quad (2)$$

where R_f is the roughness factor (the ratio of the real substrate area to its projected area) and θ is the CA on the rough surface. However, according to the Cassie-Baxter model, air can be trapped in cavities and the wetting is heterogeneous (Fig. 2b). In other words, in Cassie-Baxter state, a composite interface of solid-water-air can be formed which increases the water repellency of the surface due to partial contact area of water droplet with air. The CA is given by:

$$\cos\theta = R_f f_{\mathrm{SW}} \cos\theta_0 - (1 - f_{\mathrm{SW}}) \quad (3)$$

where f_{SW} is the solid-water fractional area.

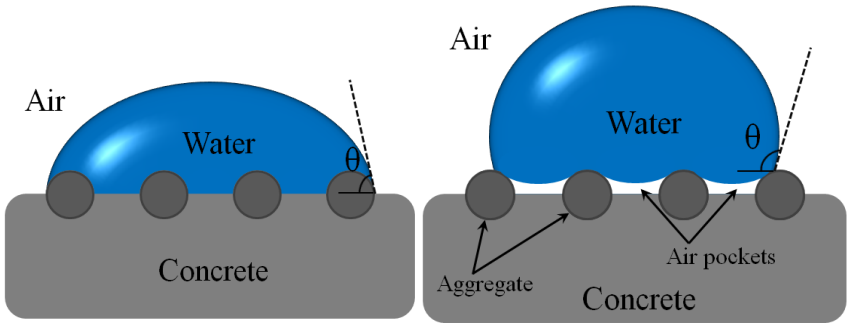

(a) (b)

Figure 2. Schematics of water droplets on the rough surfaces: (a) Wenzel (b) Cassie-Baxter

Superhydrophobic hierarchical surfaces with smaller size roughness patterns imposed over larger roughness patterns have generated interest due to their potential in industrial

applications (mainly for self-cleaning). These surfaces mimic the Lotus leaf surface, which is notorious for its superhydrophobicity and self-cleaning properties, the so-called Lotus effect. Mimicking living nature for engineering applications is called "biomimetics," and here we apply a biomimetic approach to synthesize hydrophobic concrete.[12-19]

To realize the hydrophobicity on porous materials (i.e. ceramics, concrete, etc.) it was proposed to use a siloxane based admixture containing hydrogen (e.g., polymethyl-hydrogen siloxane oil, PMHS) combined with small quantities of submicro- or nano-sized particles.[13] Randomly distributed polyvinyl alcohol (PVA) fibers embedded in the porous material and emerging from the surface can be used to achieve superhydrophobicity (Fig. 3). A modified PEHSO/PMHS admixture releases hydrogen and forms small (10 μm - 100 μm), uniform air bubbles which are evenly distributed through the concrete volume The distribution of the air bubbles through hardened concrete can be precisely tailored by preparing the water-based PEHSO emulsion with certain droplet size. The combination of the submicro- or nano-sized particles that provide the micro/nanoroughness, and fibers that introduce a hierarchical structure plays an important role in forming superhydrophobic surfaces through the hardened concrete and so improves the durability potential of concrete. The application of such emulsions for hydrophobization of concrete surfaces is a very effective solution to control the durability.[20-22] In the present paper we present a model and a systematic experimental study of various concretes prepared by the suggested methods.

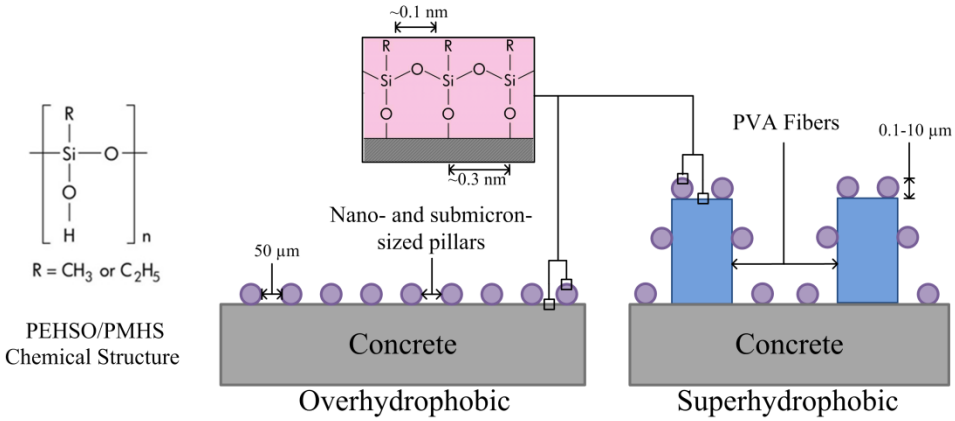

Figure 3. Schematics of the proposed "overhydrophobic" and superhydrophobic concrete

2. Modeling of superhydrophobic composites

In this section, we develop a model which relates the CA of concrete with its composition and roughness. Suppose there is a concrete surface composed of the cementitious matrix and exposed fine aggregates (sand) with the fractional areas of f_c and f_a (so that $f_c + f_a = 1$), respectively. Assume the presence of sand at the interface causes roughness so that R_{fc} and R_{fa} are roughness factors of the cementitious matrix and sand. The water CA is then given by the Cassie equation, in the form developed by Miwa[23] and Marmur[24] as

$$\cos\theta = R_{fa} f_a \cos\theta_a + R_{fc} f_c \cos\theta_c \quad (4)$$

where θ_a and θ_c are the CAs for the coated inclusions and the cementitious matrix. If water forms partial contact with the solid (Cassie-Baxter) interface the CA is given by

$$\cos\theta = R_{fa} f_a f_{AW} \cos\theta_a + R_{fc}(1 - f_a) f_{CW} \cos\theta_c + f_a f_{AW} + (1 - f_a) f_{CW} - 1 \quad (5)$$

where f_{CW} and f_{AW} are the fractional contact areas of the cementitious matrix-water and aggregate-water, respectively.

Suppose the surface composed of the cementitious matrix and exposed aggregate inclusions (sand) is coated with the hydrophobic layer. In this case, the surface energies of the matrix and reinforcement have no impact on the CA because both are coated with the layer of hydrophobic material. To optimize the aggregate fraction required to reach the desired CA ($\theta = 180°$), the following assumptions can be made: $\theta_a = \theta_c = 110°$, $f_{AW} = 1$, $R_{fa} = 2$ and $R_{fc} = 1$ and, solving the equation for the aggregates fraction, yields:

$$f_a = \frac{-0.43 f_{CW}}{-0.15 - 0.43 f_{CW}} \quad (6)$$

Figure 4(a) shows the superhydrophobic area confined between the two lines corresponding to $\theta = 150°$ and $\theta = 180°$ obtained from Eq. 6. For any point in this area, the required aggregate fractional area, f_a, and the cementitious matrix-water fractional area, f_{CW}, to achieve hydrophobic and superhydrophobicity can be calculated. Figure 4(b) illustrates the CA versus aggregate fractional area for various values of the fractional cementitious matrix-water contact area obtained from Eq. 5. The figure shows that the CA increases with increasing the aggregate fractional area as attributed to the Cassie-Baxter state.

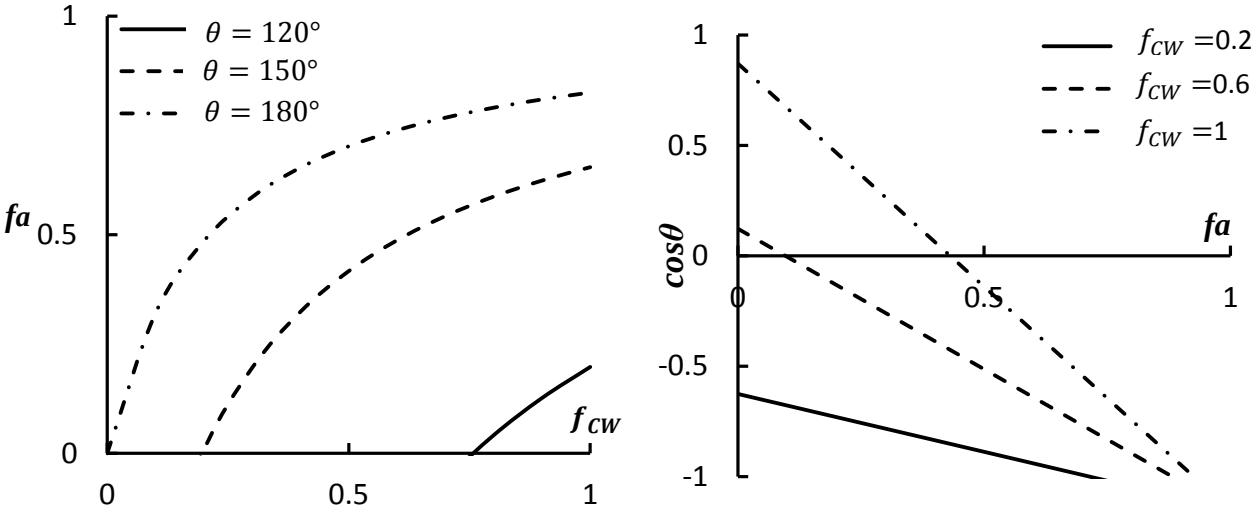

(a) (b)

Figure 4. (a) Aggregate fractional area, f_a versus the cementitious matrix fractional area, f_{CW} (b) CA versus aggregate fractional area, f_a for various values of fractional the cementitious matrix - water contact area, f_{CW}.

Suppose the distribution of the aggregates at the surface has the pattern shown in Figure 5(a). Assuming the uniform diameter, *D*, for the aggregates and the equal distance, *L*, between every two adjacent aggregates, f_a can be calculated as

$$f_a = \frac{\pi H}{L^2}(D - H) \tag{7}$$

where *H* is the projection height of the aggregates out of the surface.

The aggregate roughness factor, R_{fa} can be then calculated as

$$R_{fa} \approx 1 + \frac{\pi H}{L^2}(D - H) \tag{8}$$

Assuming $f_{AW} = \frac{2}{3} f_a$ and $f_{CW} = \frac{1}{2} f_c = \frac{1}{2}(1 - f_a)$, and then substituting Eqs. 7 and 8 into Eq. 5 yields

$$\cos\theta = \left(\frac{2\pi^2 H^2 L^2 (D-H)^2 + 2\pi^3 H^3 (D-H)^3}{3L^6}\right)\cos\theta_a - \frac{(L^2 - \pi HD + \pi H^2)^2}{2L^4} R_{fc}\cos\theta_c + \frac{7\pi^2 H^2 (D-H)^2 - 6\pi H L^2 (D-H)}{6L^4} - \frac{1}{2} \tag{9}$$

Figure 5(b) and (c) show that there is an optimal distance between the aggregates where the CA has its highest value. It is also observed that for the distances greater than the optimal distance with increasing the projection height of the aggregates, *H*, the CA increases. However,

for the distances smaller than the optimal distance when *H* increases, the CA decreases. The increase in CA with increasing the concrete roughness factor, R_{fc} is considerable.

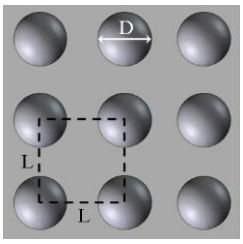

(a)

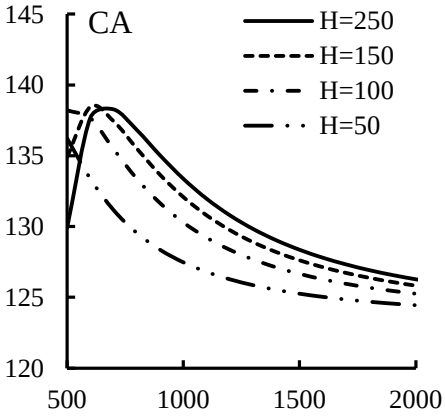

(b)

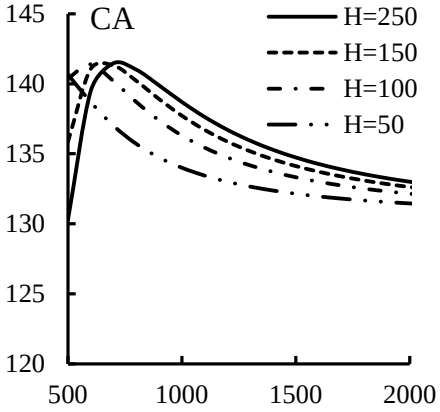

(c)

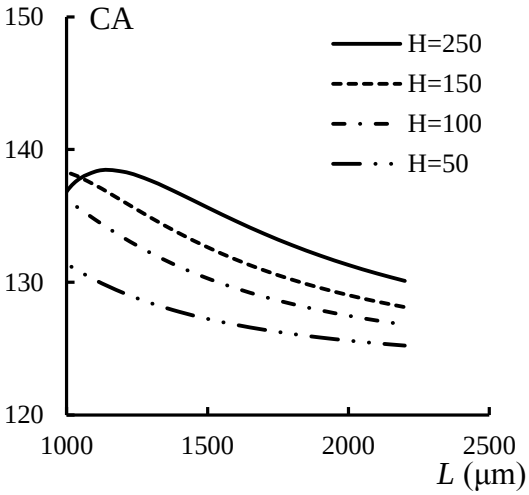

(d)

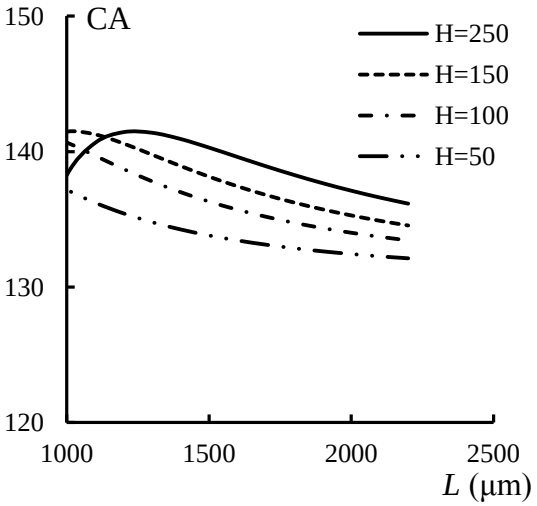

(e)

Figure 5. (a) Schematics of the aggregate patterns at the interface. (b, c, d, e) CA versus distance between the aggregates, *L*, for $\theta_a = \theta_c \approx 95°$ and (b) *D*=500 μm, R_{fc}=1 (c) *D*=500 μm, R_{fc}=3 (d) *D*=1000 μm, R_{fc}=1 (e) *D*=1000 μm, R_{fc}=3

Comparing Figures 5 (b, c) and 5 (d, e) reveals that the aggregate size affects the CA for only the shorter distances between the aggregates ($L \leq 1.5D$), while for the longer distances ($L > 1.5D$), the aggregate size does not have significant influence on the CA. Accordingly, the model facilitates design of the concrete samples in terms of aggregates contribution to achieve the higher CA as described in the following sections.

3. Materials and experimental procedures

In this section we present the experimental assessment of the hydrophobicity of mortar surfaces using different emulsion concepts (the so-called "simple," "core," and "shell" emulsions). Optical and Scanning Electron Microscope (SEM) were used to characterize the emulsions and coating treatment. The droplet size, the surface profile, along with the CA, were used as parameters to model the hydrophobicity of the specimens coated with single- and double-layers of hydrophobic emulsions; these models were compared with experimental results.

3.1. Materials

For emulsion stabilization, water soluble polyvinyl alcohol (PVA) was selected because of its nonionic character and perfect compatibility with concrete materials.[25] A highly hydrolyzed (98%) PVA with molecular weight of 16,000 from Across Chemicals was used to reduce the tendency of foam formation. Deionized water (DI water) was used as the dispersion medium for the emulsions. Polymethyl-hydrogen siloxane oil, PMHS (XIAMETER MHX-1107) from Dow

Corning with a specific gravity of 0.997 (at 25°C) and a viscosity of 30 cSt was used as hydrophobic agent. This product contains 85-100% of methylhydrogen siloxane as an active agent. Metakaolin (MK) from Burgess Optipozz or silica fume (SF) from Elkem were added to the emulsions to induce the micro roughness. The SEM (Fig.6), and the X-ray diffraction (Fig. 7) were used to analyze the morphology and phases of MK and SF. Rough and flaky particles with sizes from 0.8 to 12 μm with a certain degree of agglomeration were found in metakaolin. Silica fume was represented by spherical particles with sizes from 0.2 to 1 μm with a certain degree of agglomeration .

Mortar tiles were prepared using a commercial Type I portland cement (PC) from Lafarge. The chemical and physical properties and the X-ray diffraction of NPC are presented in Table 1 and Figure 7, respectively. ASTM C778-graded standard quartz sand with average particle size of 425 μm and tap water were used to produce mortar tiles. Polyvinyl alcohol (PVA) fibers (RECS 15x12 mm Kuralon K-II) with a diameter of 15 dtex (0.04 mm) and length of 12 mm were used in this study to achieve superhydrophobicity. These fibers had a Young's modulus of 40 GPa and a tensile strength of 1.6 GPa. The high-range water-reducing admixture (PCE) was used to improve the workability of fiber based mortar. The PCE was a commercially available polycarboxylate ether superplasticizer with a 31% solid concentration.

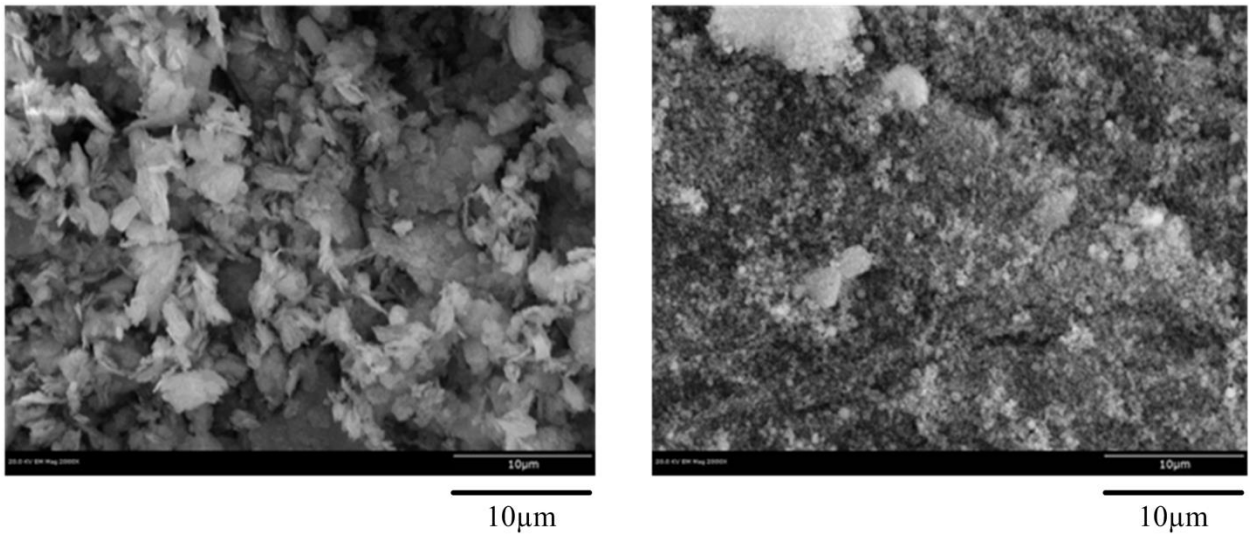

Figure 6. SEM images of metakaolin (left) and portland cement (right), (2000x magnification)

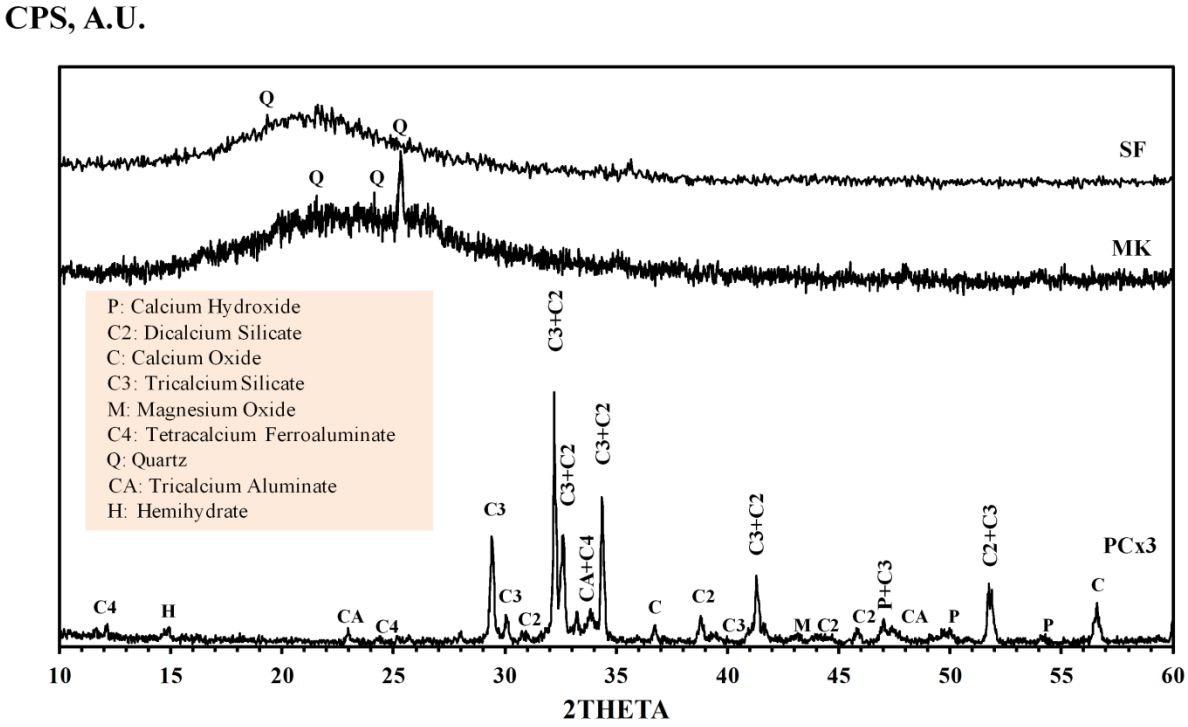

Figure 7. X-ray diffraction of SF (top), MK (middle) and PC (bottom).

Table 1. Test results of portland cement Type I compared to ASTM C150 requirements[26]

CHEMICAL	PHYSICAL

Item	Spec. Limit	Test Result
SiO_2, %		20.6
Al_2O_3, %		4.7
Fe_2O_3, %		2.7
CaO, %		63.9
MgO, %	6.0 max	2.3
SO_3, %	3.0 max	2.4
Ignition loss, %	3.0 max	2.1
Ins. residue, %	0.75 max	0.36
Free lime, %		1.1
CO_2, %		1.3
Limestone, %		3.4
$CaCO_3$ in LS, %		93.0
Potential, %		
C_3S		54.5
C_2S		17.9
C_3A		7.9
C_4AF		8.2
$C_4AF+2(C_3A)$		24.2
$C_3S+4.75(C_3A)$		93.0
Na_2O_{equi}	0.6 max	0.55

Item	Spec. Limit	Test Result
Air content, % (C-185)	12 max	7.5
Blaine fineness, m^2/kg (C-204)	260 min	380
Autoclave expansion, % (C-151)	0.8 max	0.02
Compressive strength, MPa		
1 day		12.4
3 days	12.0 min	21.7
7days	19.0 min	27.6
28 days	28.0 min	37.9
Time of setting, minutes		
Initial	45 min	110
Final	375 max	225
Heat of hydration at 7 days, kJ/kg		411
Percent Passing 325 Mesh (C-430)		95.4

3.2. Preparation of Hydrophobic and Superhydrophobic Coatings

To prepare the emulsion, water was used as a dispersion medium, water-soluble PVA as surfactant and PMHS as the dispersion phase. Metakaolin or silica fume were used to stabilize and modify the emulsion using three different approaches.[27-29] Figure 8 represents the three differences between simple, “shell” and “core” emulsion concepts that were tested. The concentration of surfactant and siloxane was kept constant at 4.4 and 25%, respectively, by the weight of the emulsion. The water-soluble PVA swells quickly in water and then clumps together. To avoid clumping, it was gradually added to de-ionized water and stirred for 10 minutes at 23±3°C, using a magnetic stirrer with a hot plate. Then, to achieve a complete dissolution, temperature was increased to 95±2.5°C, and kept constant for 40 minutes while stirring. The solution was allowed to cool in a water bath until temperature of 23±3°C was achieved. The mixing procedure of PHMS and metakaolin/silica fume in PVA solution is explained in Figure 9.

The proportions of metakaolin or silica fume to achieve "overydrophobic" and superhydrophobic surfaces were 0.5 and 5.0% by weight of emulsion, respectively. High speed mixer (HSM, model L5M-A from Silverson) was used to prepare the emulsions. To stabilize the plain emulsions (without particles), a high speed/shear mixed at 10,000 rpm was used to produce the small droplet size. Medium speed (5000 rpm) was used only when particles were added. The emulsions were characterized by an optical microscope (Olympus BH-2) at 1000x magnification.

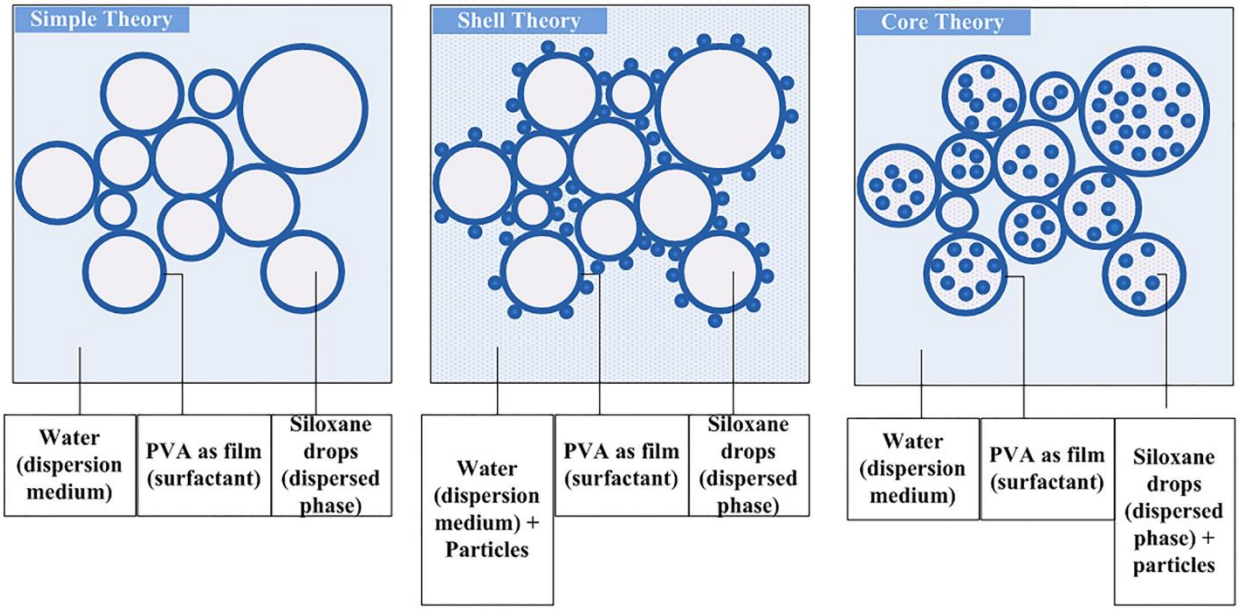

Figure 8. The explanation of simple, core and shell concepts used to design PMHS emulsions

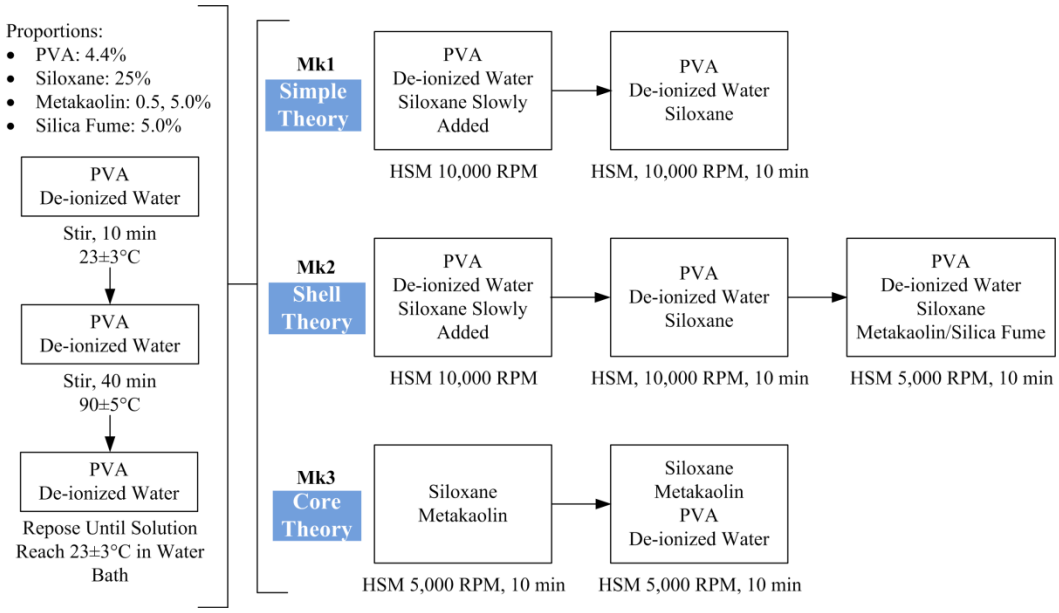

Figure 9. The procedure for preparation of PHMS emulsions

3.3. Sample Tile Preparation

Standard mortar (ASTM C109)[30] tiles of 10 × 10 × 5 mm were prepared for test on hydrophobicity using water to cement ratio (W/C) of 0.5 and sand to cement ratio (S/C) of 2.75. Tiles were cast and compacted using a vibrating table at 150 Hz for 20 seconds. Tiles were allowed to harden for 24 hours at 23±3 °C and at least 90% of relative humidity. After 24 hours, tiles were de-molded and the surface was roughened with a silicon carbide grinding paper with a grit of 320 for 1 minute in order to expose the fresh surface and sand aggregates. High porosity and scratches revealed on the specimens after this procedure. The porosity of non-covered specimens is shown at different magnifications in Figure 10. A soft brush and water were used to remove any loose particles from the tile surface. Tiles were allowed to dry for 24 hours at 40±2 °C and after this were exposed to room conditions for 24 hours. The tiles were immersed into the PHMS emulsion for 20 seconds. Excess emulsion from the tiles was removed using a soft plastic

spatula. Specimens were dried at a room temperature for 48 hours. This procedure was repeated when two coating layers were required.

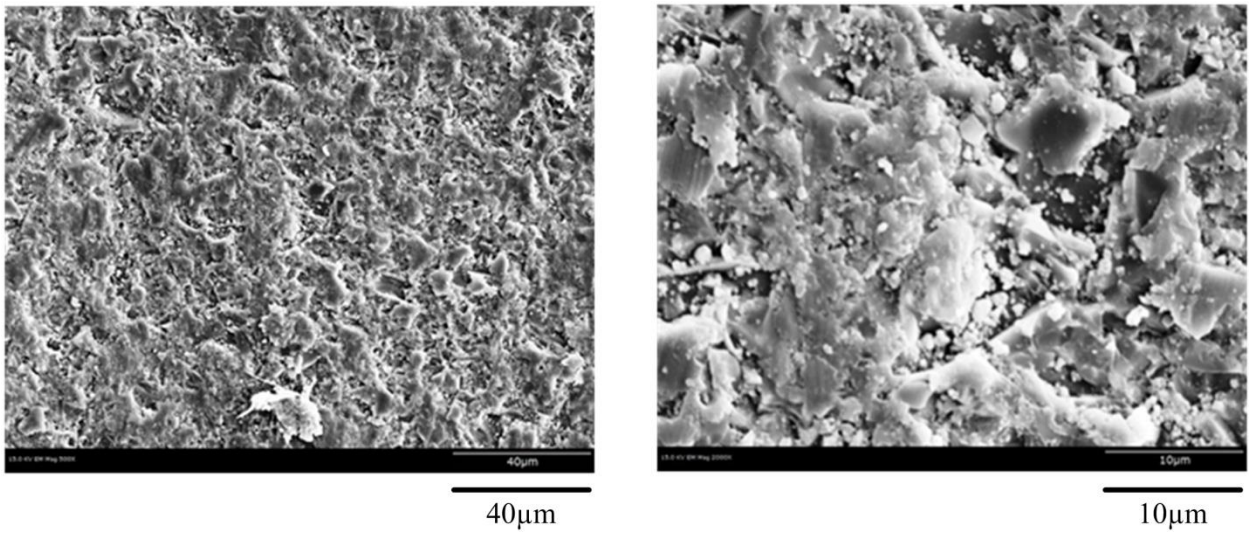

Figure 10. The surface of mortar tiles observed by SEM at 500x (left) and 2000x (right) magnifications.

For superhydrophobic tiles, the standard (ASTM C109)[30] mortar was produced with 1% (by the volume of the total mix) of PVA fibers. Superplasticizer at a dosage of 0.1% (of solid content by weight of portland cement) was used to provide required workability level. After hardening, the surface of the tiles was roughened with a silicon carbide grinding paper with a grit of 60 for 30 seconds in order to expose the fresh surfaces, fibers and sand aggregates. Polished tiles were washed with tap water to remove any contamination from the surface. An ultrasound processor UIP1000hd was used at 50% of maximum power for 60 seconds to remove any loose particles from the surface of the tiles. Specimens were placed in an oven at 40 °C for 24 hours to remove any excess of water.

4. Results and Discussion

4.1. Characterization of Coatings

The droplet sizes and the dispersion of metakaolin in the emulsions are shown in Figure 11. Emulsion Mk1 (Fig. 11a) is mainly presented by uniform droplets of approximately 2 µm with few inclusions of larger droplets (<20 µm). Emulsion Mk2 (Fig. 11b) is presented by well-distributed droplets with sizes from 3 to 30 µm. Particles of metakaolin were found on droplet boundaries. Emulsion Mk3 (Fig. 11c) is mainly presented by well-distributed droplets with sizes from 2 to 5 µm with some inclusions of larger droplets (<40 µm). In this emulsion, the metakaolin particles were found to be embedded within the droplets.

These three emulsions successfully represent the proposed concepts detailed in Figure 8. The speed selected allows the formation of an emulsion with small droplets (Fig 11.a), which is one of the key parameter for the stability of the emulsion.[31] Due to its hydrophilic surface,[32,33] metakaolin/silica fume particles increase the coalescence of the emulsion during the mixing procedure, acting as an attraction force that combines the smallest droplets observed in Figure 11(a), into bigger droplets observed in Figure 11(b). Contrary to Mk2 emulsions, encapsulated particles of metakaolin in the oil-phase of Mk3 emulsion (Fig. 11.c), prevented the droplets from coalescence.

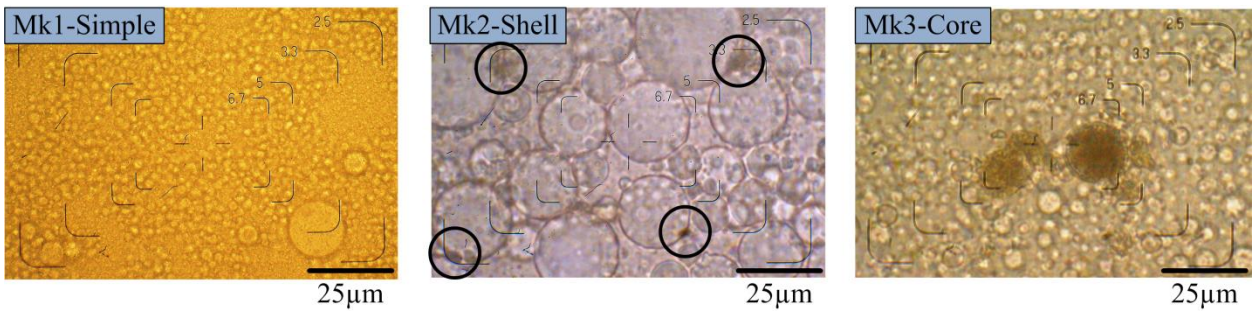

(a) (b) (c)

Figure 11. Emulsion images taken by optical microscope at 1000x magnification for: (a) Mk1; (b) Mk2; and (c) Mk3; with metakaolin particles.

The morphology of two-layer superhydrophobic coatings was analyzed by SEM technique (Fig. 12) in order to understand the effects of emulsion type and surface treatment. The coatings on these specimens are directly related to the method that was used to produce the emulsions. Irregular surface structure is produced by collapsed bubbles with the size of 3 to 13μm and by smaller bubbles of 1 to 2.5μm as observed for Mk1 coating (Fig. 12a). The collapsed bubbles are dominating in Mk1 sample, it can be concluded that the simple emulsion (Fig. 8) had no capability of preserving the bubble structure on a surface resulting in the appearance of "moon craters". The Mk2 coating (Fig. 12b) appears to mimic the relief of the surface, leaving a uniform foam free self-assembled particle coating a "bump" size of 0.5 to 8μm. The Mk3-core emulsion with incorporated particles allows the formation of "intact" bubbles reinforced by MK particles as a coating structure. Bubbles of 0.5 to 22 μm remained on the surface of the specimens and some collapsed bubbles of 1 to 19 μm can be observed on these coatings (Fig. 12c). At higher magnification (Fig. 12d), Mk2 surface reveals the bubble formation of the coating due to the first coating application. With the second application of Mk2 emulsion covers the voids left by the irregularities of the tile surface (Fig. 10) and partially cover the bubbles and particles (Fig. 12d).

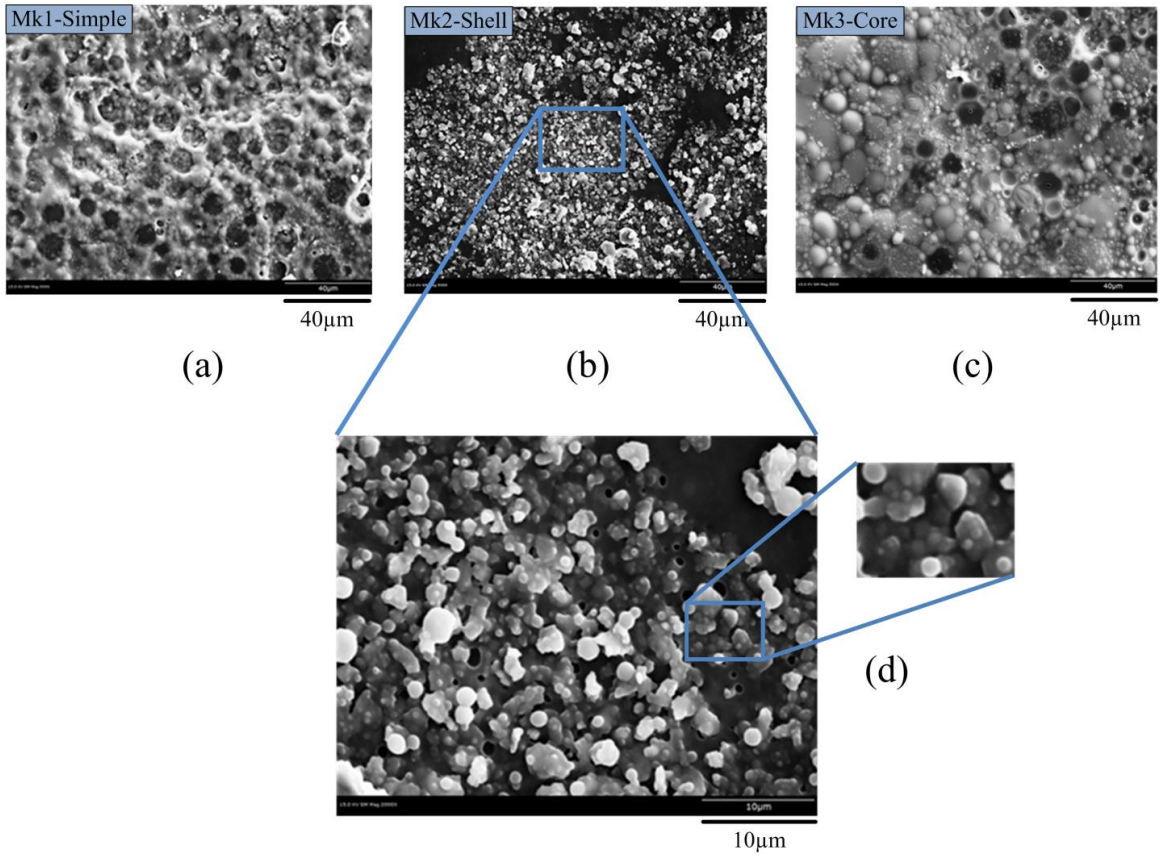

Figure 12. SEM images of superhydrophobic coatings at 500x magnification for: a) Mk1; b) Mk2; c) Mk3; and d) Mk2 at 2000x magnification.

To understand the effect of droplet size in the emulsion on the irregularities of hydrophobic surface coating, the maximum and minimum diameters of droplet size and intact or collapsed bubbles were determined. Emulsion droplets and intact or collapsed bubbles were considered of spherical shape. The effect of the droplet size of the emulsion on surface irregularities is demonstrated in Figure 13. As a general trend, the bigger the droplet size is, the bigger the diameter of the bubble. Collapsed surface structure (Mk1-Simple) requires a small increment on the droplet size in order to increase the irregularities on the surface. From this analysis, to produce small "moon craters" a higher speed during the emulsion production is required,. Bigger intact bubbles (Mk3-Core) can be realized when the emulsion droplet size is

large (>30 μm). However, intact bubble structure is difficult to realize since the larger droplets result in unstable emulsions. Here, the addition of particles increase the stability of emulsions and reinforce the bubbles.

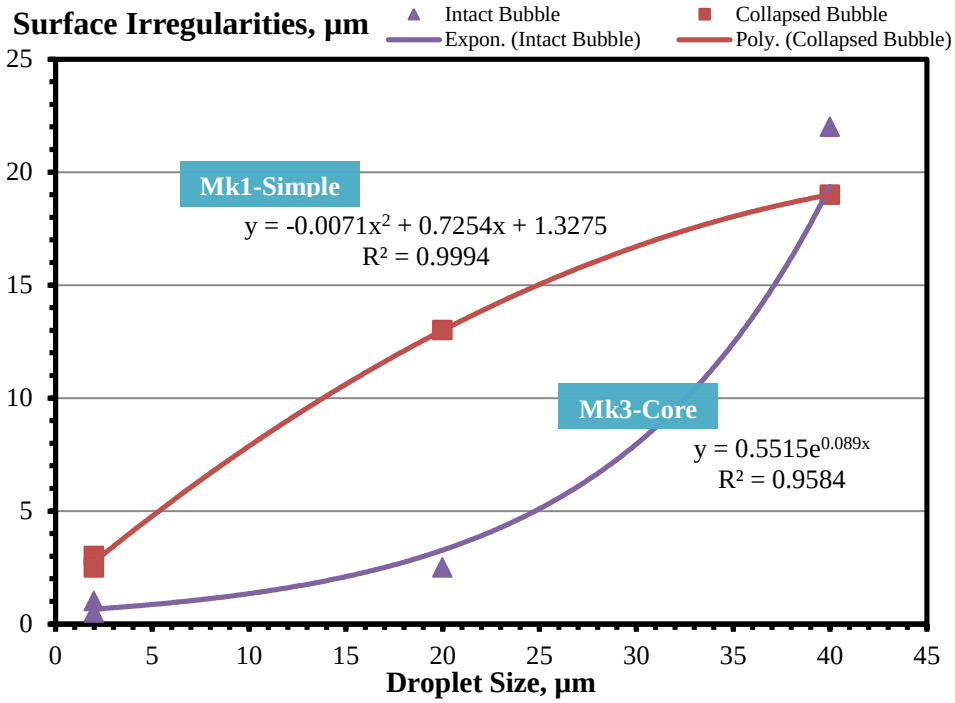

Figure 13. The effect of the droplet size on the irregularity of the coatings.

4.2. Contact Angle Measurement

The wetting properties of the tiles were examined by measuring the water CA using the Ramé-Hart Goniometer model 250. At least three, 5μl water droplets were placed at different points on each sample. The siloxane based emulsion with 0.5% of metakaolin was used to achieve hydrophobicity. The values of water CAs as well as the images of water droplets on different hydrophobic coatings are shown in Figure 14. It was found that the CAs of all coated specimens increased by more than 120% vs. the reference material. The application of a second coating did not improve the performance of Mk1 and Mk3. Apparently, the hydrophobic first

coat of Mk1 and Mk3 did not allow for the settlement of the second coat. A remarkable performance of self assembled Mk2 was observed, not only on single-coated specimens (with CA of 3 times better vs. the reference), but also for double-coated specimens (CA of 3.5 times the reference). Metakaolin particles, located at the boundaries of the droplets, acted as support for the second coating, providing the surface a micro-roughness and increasing the hydrophobicity to the "over-hydrophobic" range.

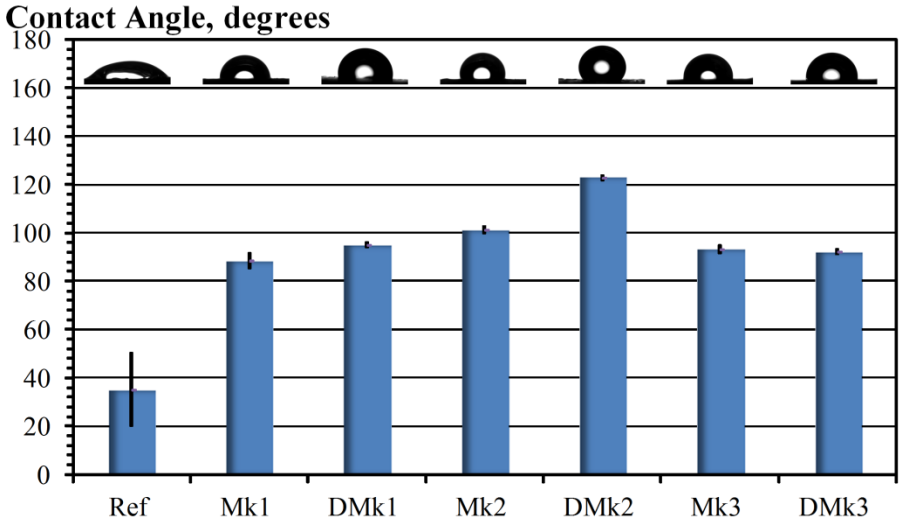

Figure 14. The contact angle of specimens with single (Mk)- and double (DMk)- coatings.

The specimens with randomly distributed PVA fibers, emerging from the surface were coated with the siloxane based emulsion Mk2 with 0.5 and 5.0% of metakaolin (Mk2-MK-0.5 and Mk2-MK-5, respectively) and 5.0% of silica fume. Coated surfaces were compared with an uncoated tile. With the use of PVA fibers, the CA of Mk2 specimen was enhanced from 101.3 to 128.2 degrees (Mk2-MK-0.5), Figure 14. In this way, PVA fibers can be used to increase the hydrophobic effect by 26% over (over plain tiles). The combination of the submicron-sized particles which provide the micro and nano- roughness, and fibers which introduce a hierarchical

structure enable to achieve the superhydrophobic effect as observed on specimens with 5.0% of particles. The use of higher volume of particles enables , the further increase of CA. The superhydrophobic behavior was confirmed by the roll-off angle tests, in which specimens with higher CA had lower roll-off angle (Fig. 15). In this way, the use of exposed fiber surfaces and emulsions with high volumes of particles (5% of silica fume or metakaolin) can induce the superhydrophobic performance.

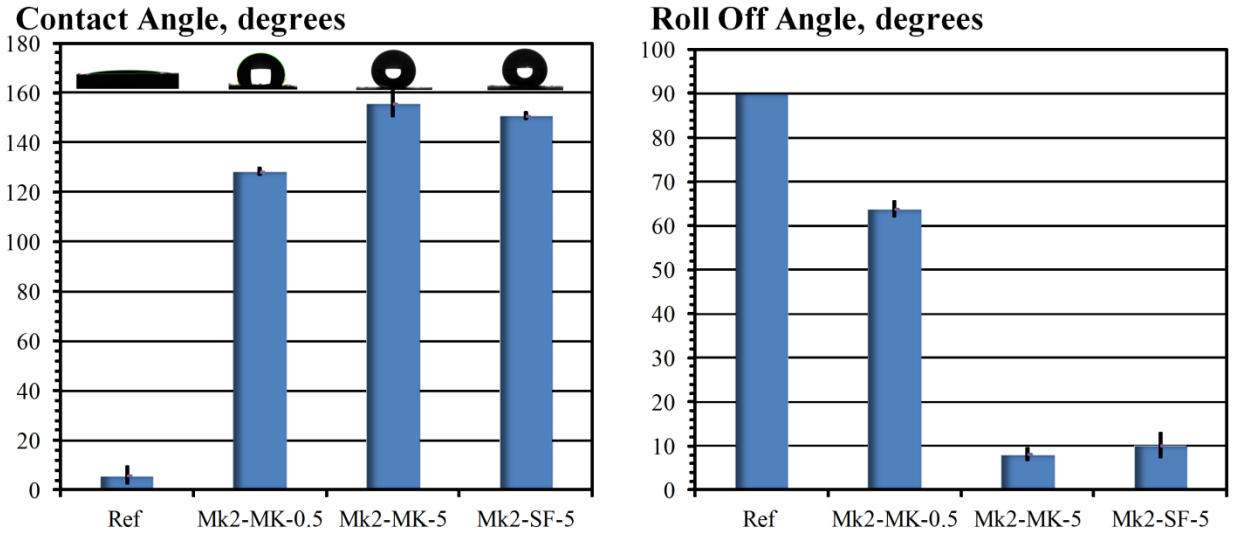

Figure 15. The contact and roll off angle of specimens with single (Mk)- and double (DMk)-coatings.

4.3 Contribution of Hierarchical Roughness

To calculate the water CA on the surface of the concrete with dual scale or hierarchical roughness, induced by micron-sized bubbles or MK particles, the smaller scale roughness needs to be considered in proposed models. Introducing the R_{fs} as the second order roughness induced by cellular structure or particles on the surface (Fig. 16), CA can be calculated as

$$\cos\theta = \frac{2\pi^2H^2}{3L^4}(D-H)^2(R_{fa}+R_{fs})\cos\theta_a + \frac{(L^2-\pi H(D-H))^2}{2L^4}(R_{fc}+\frac{L}{D}R_{fs})\cos\theta_c + \frac{7\pi^2H^2(D-H)^2-6\pi HL^2(D-H)}{6L^4} - \frac{1}{2} \quad (10)$$

According to Figure 5, the value of R_{fs} for the aggregates with D=500 μm can be assumed as

$$R_{fs} = \frac{n\pi d^2}{L^2} \quad (11)$$

where n is the number of bubbles in D=500 μm (Fig. 16) and d is the diameter of the bubbles or particles (protrusions) on the surface.

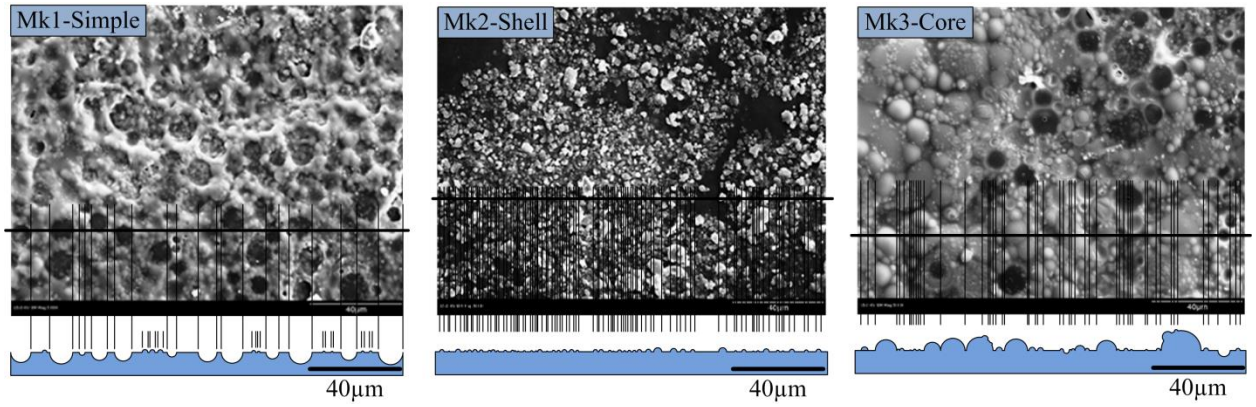

(a) (b) (c)

Figure 16. The profile of surfaces of mortar specimens: (a) Collapsed cellular structure, (b) particle coating, (c) bubbles on the surface.

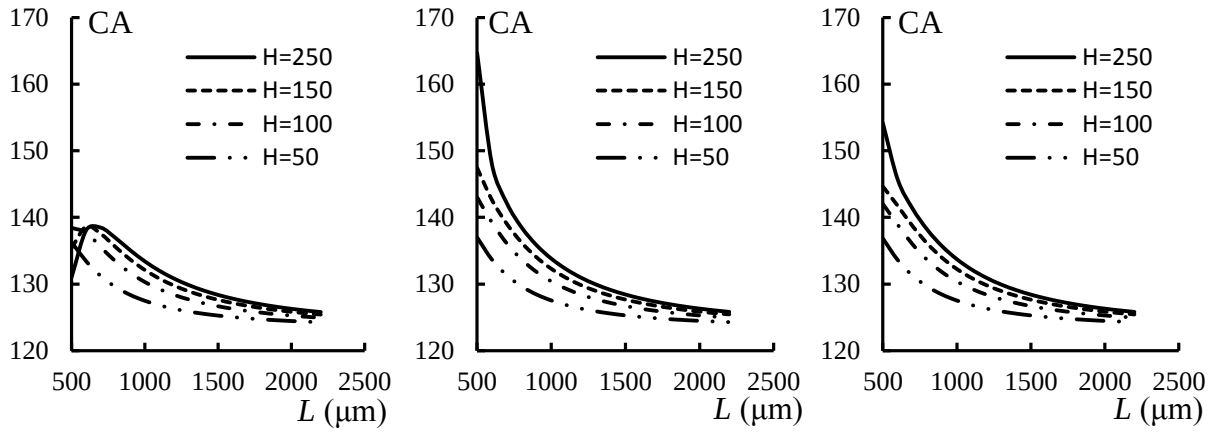

Figure 17. CA versus distance of the aggregates, *L*, for *D*=500 μm, R_{fc}=1 and $\theta_a = \theta_c \approx 95°$ (a) n=30 and d=2 μm (Mk1) (b) n=100 and d=5 μm (Mk2) (c) n=20 and d=10 μm (Mk3)

Figure 17 shows the water CA versus *L* for the aggregates with *D*=500 μm. According to Figure 16, it is assumed that *n*=30 and *d*=2 μm for collapsed cellular structure sample (Mk1), *n*=100 and *d*=5 μm for particulate self-assembled coating (Mk2) and *n*=20 and *d*=10 μm for bubble coated sample (Mk3). It is observed that the CAs of Mk2 coated samples are higher than those of Mk1 and Mk3 samples. It occurs due to the higher number of micron-sized particles present at the surface of Mk2 coated samples comparing to cellular and bubble coatings. It is also observed that with increasing the projection height of the aggregates, *H*, the CA increases.

5. Conclusions

The technology of hydrophobic emulsions and their application on portland cement mortar tiles were investigated. A theoretical model was developed and a relationship between the droplet size and the size of irregularities on the surface of coating were established to optimize the design of the emulsions. The models for coated and non-coated concrete that can be

generalized for other types of materials were developed. An optimal distance between the aggregates where the CA has the highest value was predicted based on proposal models. The effect of dual scale roughness of concrete surface on CA was theoretically investigated. The introduction of hierarchical roughness and chemical modification of the surface can be beneficial for the design of bioinspired superhydrophobic concretes.

The proposed emulsion types were successfully realized by using different mixing procedures. Wetting of mortar tile surfaces by water was investigated experimentally. PVA fiber mortar tiles coated with the Mk2-MK-5 solution showed the highest water-repellency due to its hierarchical surfaces and hydrophobization.

In summary, we reported an innovative method to produce “over-hydrophobic” and superhydrophobic water-repellent concrete with water CAs reaching superhydrophobicity values and low roll-off angles. Water-repellent concrete can have numerous applications in construction and civil engineering due to its enhanced durability.

Acknowledgements

The authors acknowledge and appreciate the financial support from the National Center for Freight and Infrastructure (CFIRE), the National Science Foundation (NSF) and the Research Growth Initiative (RGI). Special thanks to the Advanced Analysis Facility (AAF) at the University of Wisconsin-Milwaukee for assistance with the XRD and SEM studies.

References

(1) Stefanidou, M.; Matziaris, K.; and Karagiannis, G. *Geosciences* **2013**, *3*, 30-45.

(2) Sobolev, K.; Flores, I.; Hermosillo, R.; and Torres-Martínez L.M. In *Proceedings of the ACI Session on Nanotechnology of Concrete: Recent Developments and Future Perspectives*, edited by Sobolev, K. and Shah, S. P. Denver, CO, **2008**, ACI SP-254, 93-120.

(3) Marmur, A. "A guide to the Equilibrium Contact Angle Maze" In *Contact Angle Wettability and Adhesion*; ed. by K. L. Mittal, Brill/VSP, Leiden, **2009**; Vol. 6, p 3-18.

(4) Bormashenko, E., *Wetting of Real Surfaces*; Walter de Gruyter & Co, Berlin **2013**, p 170.

(5) Bormashenko, E.; Pogreb, R.; Whyman, G.; Bormashenko, Y.; Erlich, M. *Appl. phys. Lett*. **2007**, *90*, 201917.

(6) Li, W.; and Amirfazli, A. *Soft Matter*, **2008**, *4*, 462-466.

(7) Choi, C.-H.; Kim. C.-J. *Langmuir* **2009**, *25*, 7561-7567.

(8) Tadmor, R.; Bahadur, P.; Leh, A.; N'guessan, H.E.; Jaini, R.; Dang, L. *Phys. Rev. Lett.* **2009**, *103*, 266101.

(9) N'guessan, H. E.; Leh, A.; Cox, P.; Bahadur, P.; Tadmor, R.; Patra, P.; Vajtai, R.; Ajayan, P. M.; Wasnik, P. *Nature Communications* 2**012**, *3*, 1242.

(10) Wenzel, R. N. *Ind. Eng. Chem*. **1936**, *28*, 988–994.

(11) Cassie, A. B. D.; and Baxter, S. *Trans. Faraday Soc.* **1944**, *40*, 546–551.

(12) Sobolev, K.; and Ferrada-Gutiérrez, M. *American Ceramic Society Bulletin* **2005**, *11*, 16-19.

(13) Sobolev, K.; and Batrakov, V. *ASCE Journal of Materials in Civil Engineering* **2007**, *19*, 809-819.

(14) Kietzig, A. M.; Hatzikiriakos, S. G.; Englezos, P. *Langmuir* **2009**, *25*, 4821.

(15) Nosonovsky, M. *Langmuir* **2007**, *23*, 3157-3161.

(16) Nosonovsky, M. *Nature* **2011**, *477*, 412-413.

(17) Nosonovsky, M.; and Bhushan, B. *Current Opinions Coll. Interface Sci*. **2009**, *14*, 270-280.

(18) Nosonovsky, M.; Hejazi, V.; Nyong, A. E.; Rohatgi. P. K. *Langmuir* **2011**, *27*, 14419–14424.

(19) Hejazi, V.; Sobolev, K.; Nosonovsky, M. *Nature's Sci. Rep*. **2013**, *3*, 2194.

(20) Sobolev, K.; Tabatabai, H.; Zhao, J.; Flores, I.; Muzenski, S.; Oliva, M.G.; Rauf, R.; Rivero, R. *CFIRE Phase I* **2013**, 04-09 May.

(21) Sobolev, K.; Tabatabai, H.; Zhao, J.; Flores, I.; Muzenski, S.; Oliva, M.G.; Rauf, R.; Rivero, R. *CFIRE Phase II* **2013**, 05-10 June.

(22) Muzenski, S.W.; Flores-Vivan, I.; Beyene, M.A.; Sobolev, K. *Transportation Research Board* **2014**, 93rd Annual Meeting, Washington, D.C., (Submitted).

(23) Miwa, M.; Nakajima, A.; Fujishima, A.; Hashimoto, K.; Watanabe, T. *Langmuir* **2000**, *16*, 5754–5760.

(24) Marmur, A. *Langmuir* **2003**, *19*, 8343–8348.

(25) Kim, J. H.; and Robertson, R. E. *Cement and Concrete Research* **1999**, *29*, 407-415.

(26) ASTM C 150, *American Society for Testing and Materials; Standard specification of portland cement*, ASTM C 150-12, *2012*, 4.01.

(27) Binks, B. P.; and Lumsdon, S. O. *Langmuir* **2000**, *16*, 8622-8631.

(28) Aveyard, R.; Binks, B.P.; Clint, J.H. *Advances in Colloid and Interface Science* **2003**, *100-102*, 503-546.

(29) Ngai, T.; Auweter, H.; and Behrens, S.H. *Macromolecules* **2006**, *39*, 8171-8177.

(30) ASTM C 109, *American Society for Testing and Materials; Compressive Strength of Hydraulic Cement Mortars* (Using 2-in or 50-mm Cube Specimens), ASTM C 109-12, **2012**, 4.01.

(31) Charles Ross & Son Company, Improve emulsion stability through ultra-high shear mixing, Mixing Technology Insight, http://www.mixers.com/insights/mti_17.pdf

(32) Barnes, P.; Bensted, J. *Taylor & Francis*, London **2002**, Edition 2, Nov 1.

(33) Dhir, R.; Hewlett, P. *Taylor & Francis*, **2003**, *4*, 758.

Table of contents/Abstract graphics

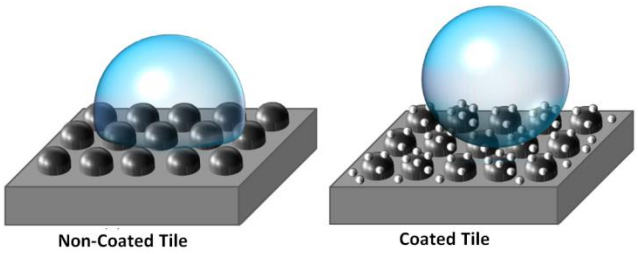

Video of water droplet on superhydrophobic concrete

stored at googledrive

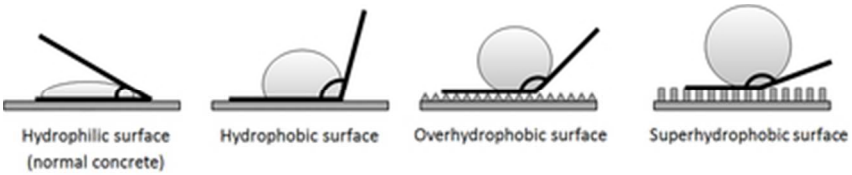

35x7mm (300 x 300 DPI)

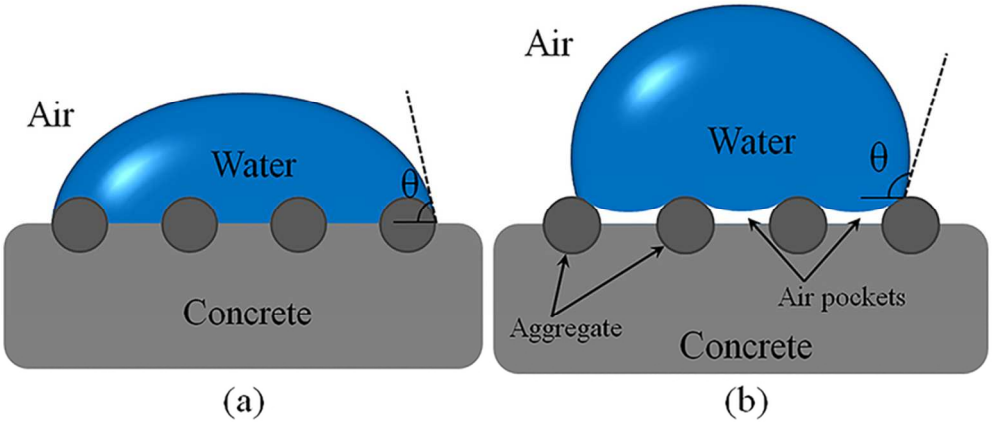

75x32mm (300 x 300 DPI)

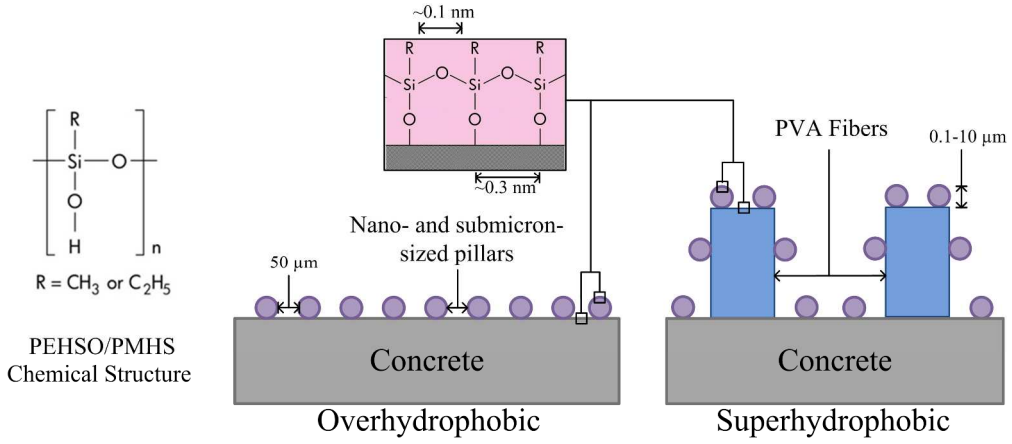

266x117mm (300 x 300 DPI)

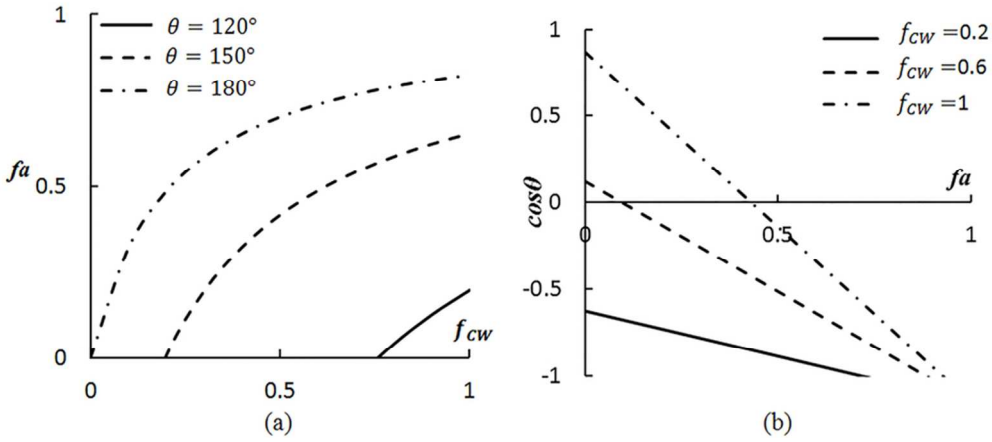

78x35mm (300 x 300 DPI)

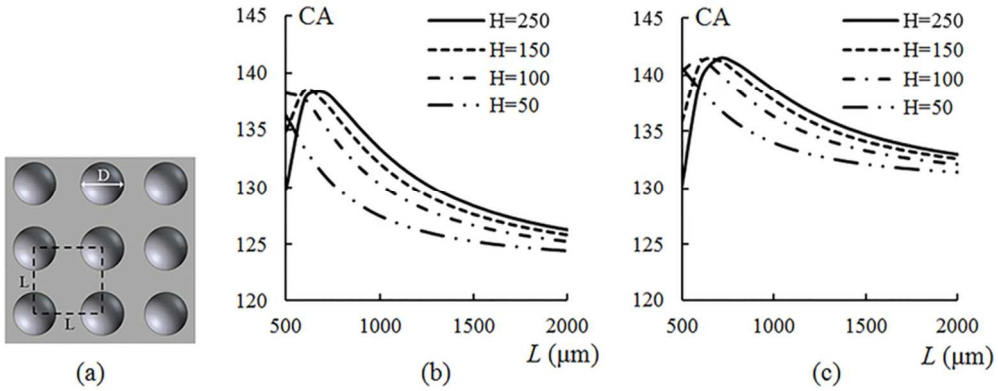

71x28mm (300 x 300 DPI)

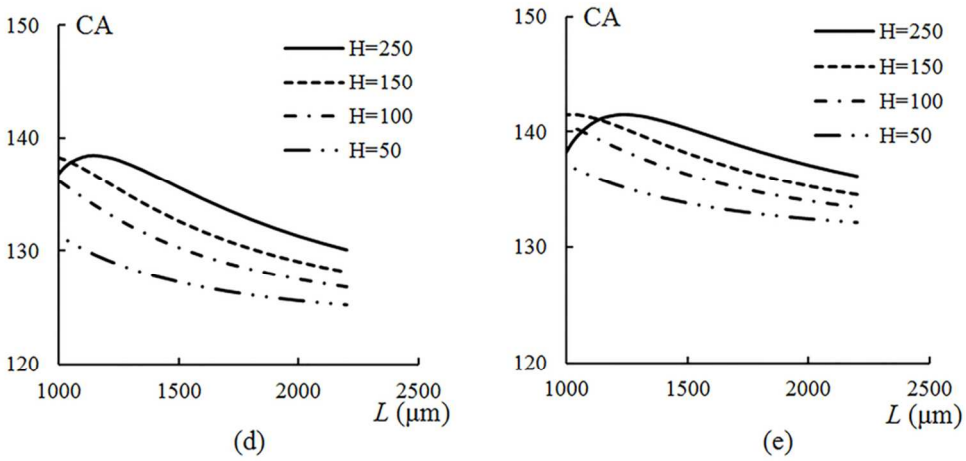

83x39mm (300 x 300 DPI)

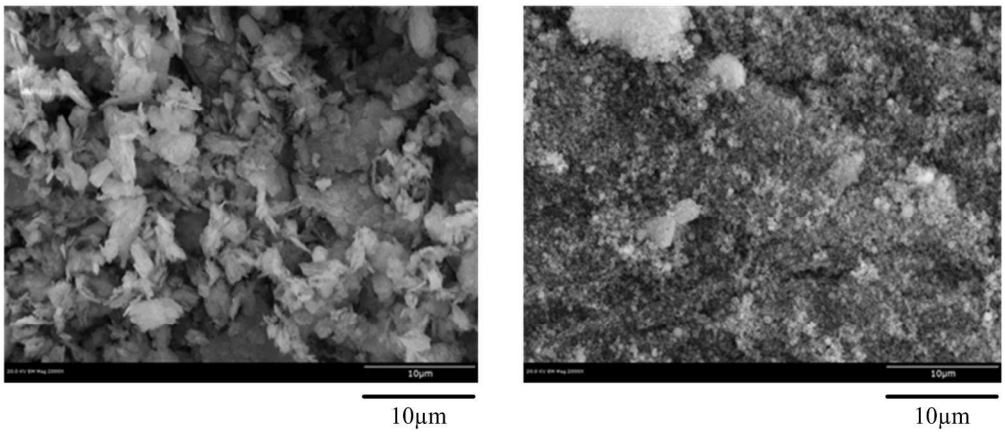

265x113mm (300 x 300 DPI)

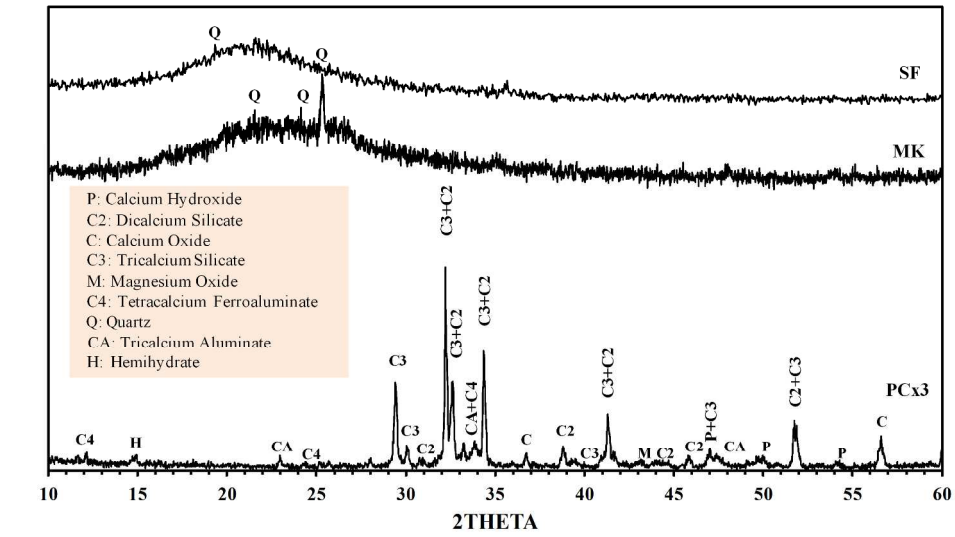

261x159mm (300 x 300 DPI)

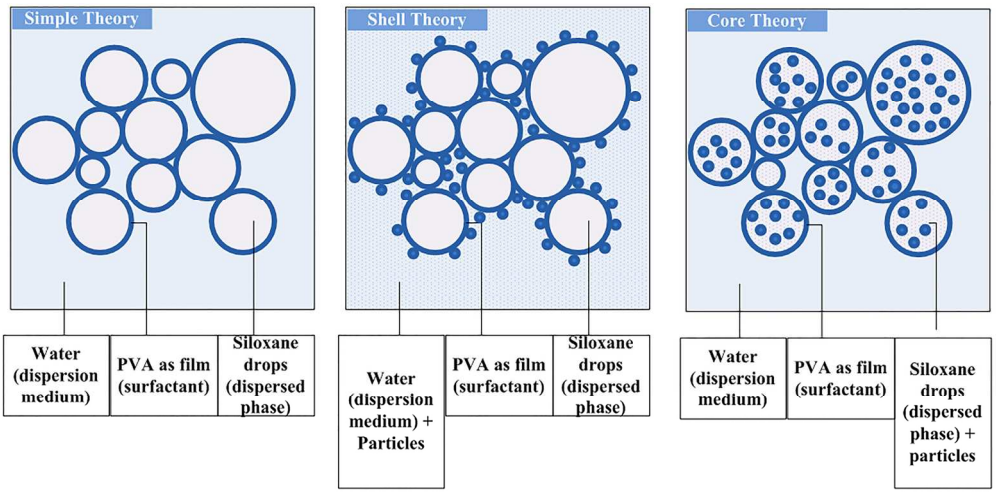

177x87mm (300 x 300 DPI)

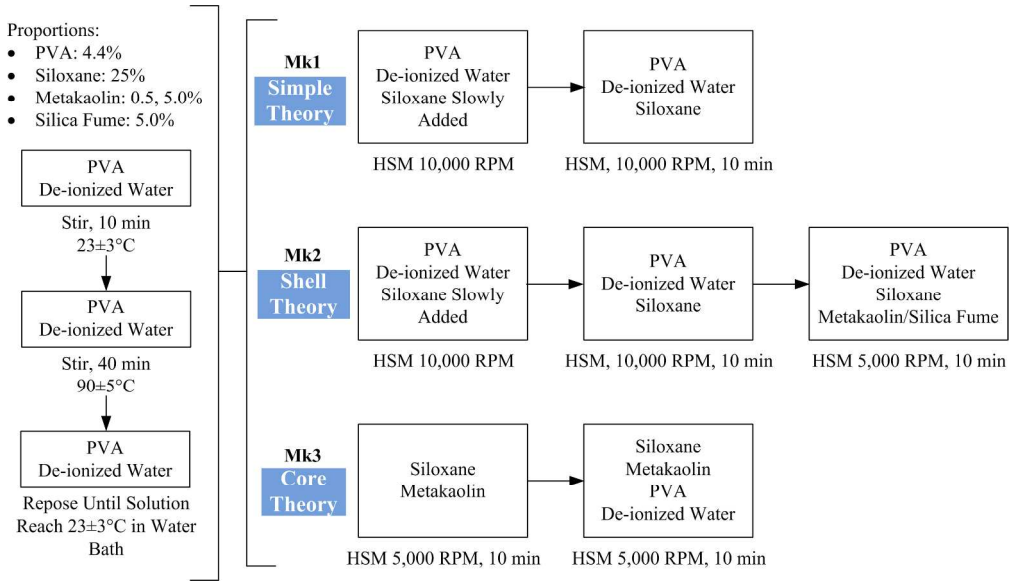

225x129mm (300 x 300 DPI)

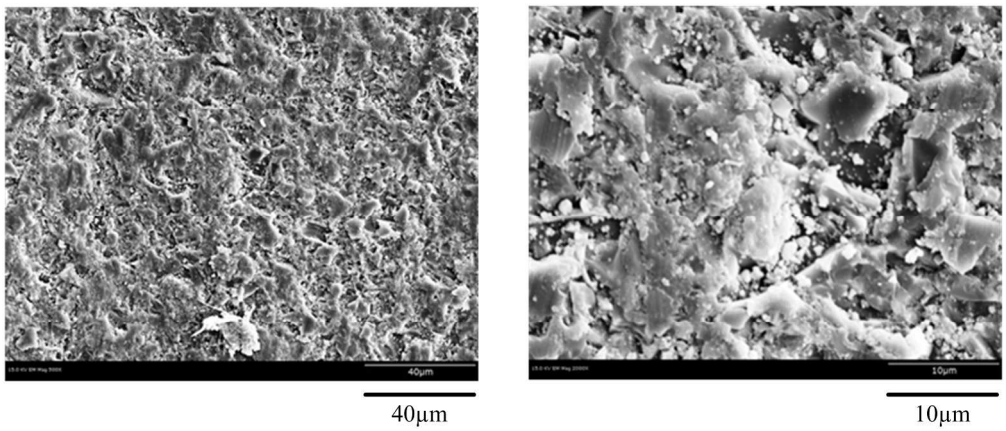

266x113mm (300 x 300 DPI)

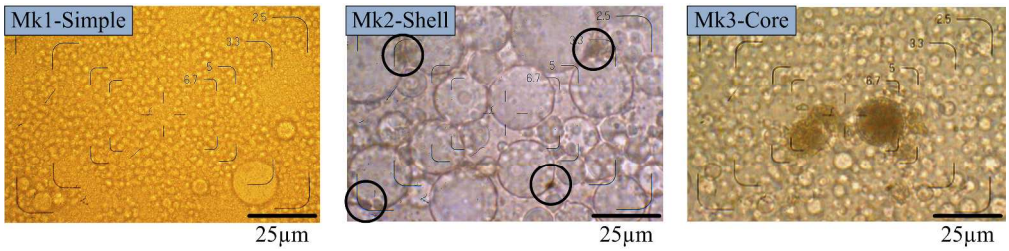

279x68mm (300 x 300 DPI)

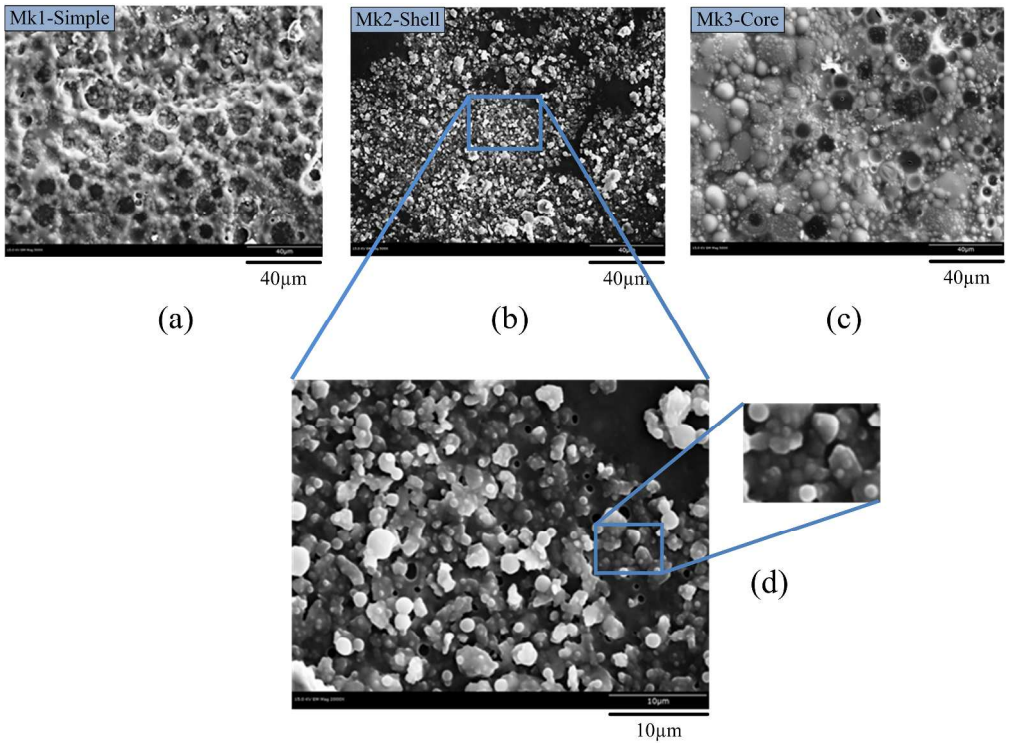

321x237mm (300 x 300 DPI)

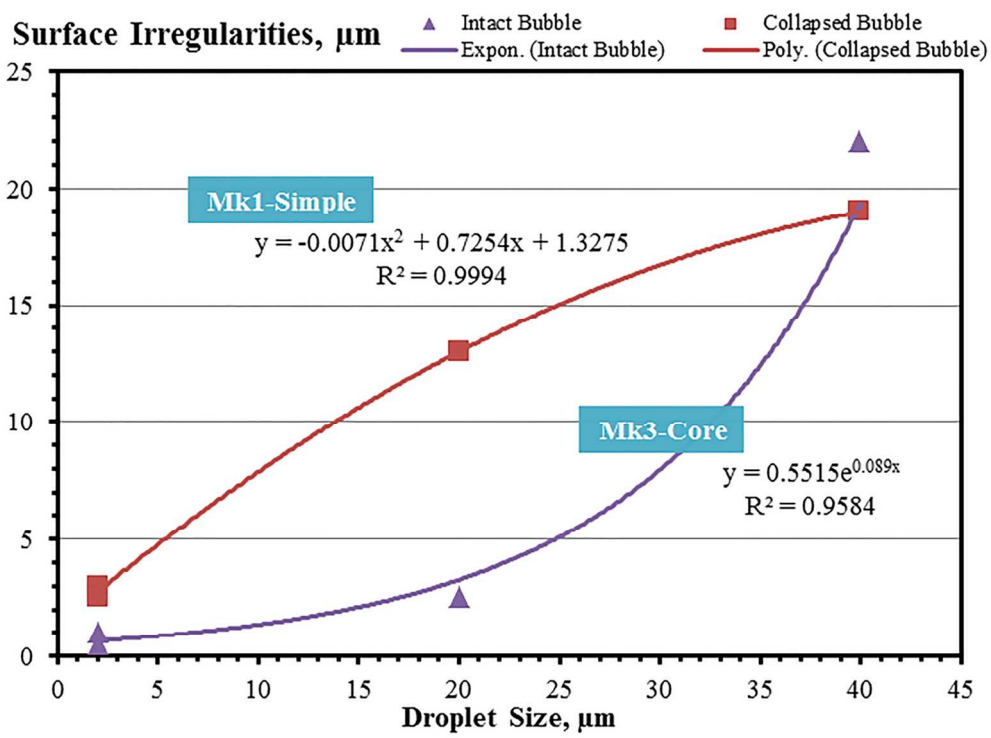

130x96mm (300 x 300 DPI)

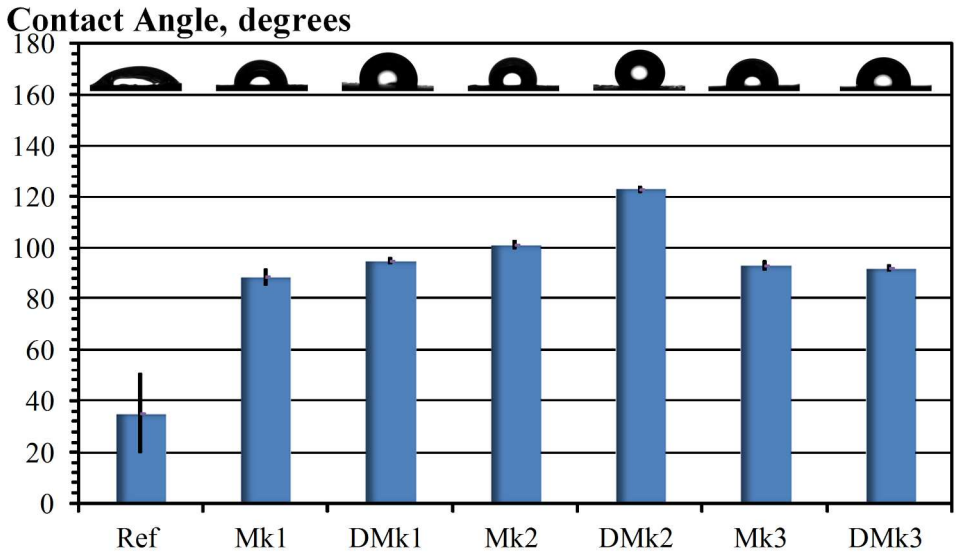

201x117mm (300 x 300 DPI)

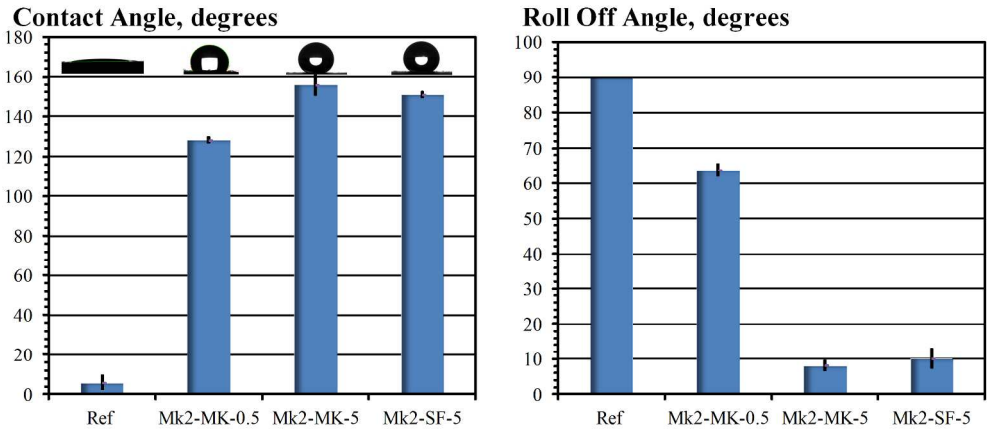

262x118mm (300 x 300 DPI)

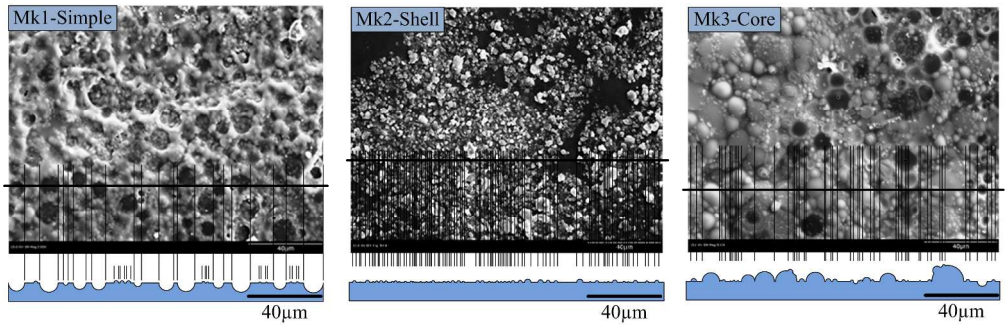

324x104mm (300 x 300 DPI)

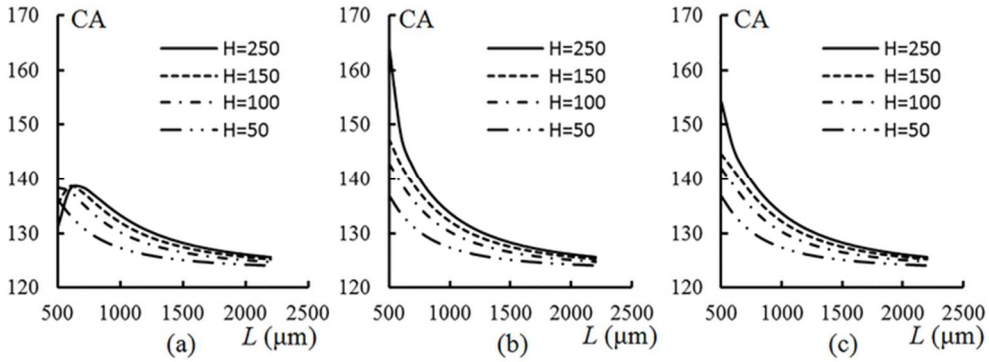

65x23mm (300 x 300 DPI)

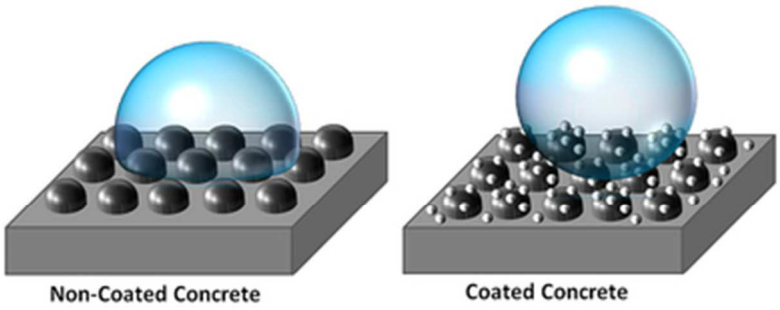

32x12mm (300 x 300 DPI)